Bayesian-based Localization of Wireless Capsule Endoscope using Received Signal Strength

Esmaeil S. Nadimi, *member IEEE*, Victoria Blanes-Vidal, Vahid Tarokh, *Fellow IEEE,* and Per Michael Johansen

***Abstract*—In wireless body area sensor networking (WBASN) applications such as gastrointestinal (GI) tract monitoring using wireless video capsule endoscopy (WCE), the performance of out-of-body wireless link propagating through different body media (i.e. blood, fat, muscle and bone) is still under investigation. Most of the localization algorithms are vulnerable to the variations of path-loss coefficient resulting in unreliable location estimation. In this paper, we propose a novel robust probabilistic Bayesian-based approach using received-signal-strength (RSS) measurements that accounts for Rayleigh fading, variable path-loss exponent and uncertainty in location information received from the neighboring nodes and anchors. The results of this study showed that the localization root mean square error of our Bayesian-based method was 1.6 mm which was very close to the optimum Cramer-Rao lower bound (CRLB) and significantly smaller than that of other existing localization approaches (i.e. classical MDS (64.2mm), dwMDS (32.2mm), MLE (36.3mm) and POCS (2.3mm)).**

I. Introduction

The lifetime chance of developing colorectal cancer (3rd most common cancer worldwide) is 1 in 20. More than 80% of colorectal cancers arise from polyps, making this cancer amenable to screening [1]. Early detection and screening of these polyps reduce the colorectal cancer deaths by 60%. This statistic indicates that effective advancements in endoscopy technology are extremely worthy of investigation. Recently, wireless capsule endoscopy (WCE), a disposable and ingestible wireless micro-robot that allows for direct and noninvasive visual examination of the inner lining of the GI tract has been developed. The capsule is equipped with miniature cameras on both ends and is about the size of a multi-vitamin pill, which can be swallowed easily. Sensor arrays are strategically placed on the patient's chest and connected to a data recorder, worn on a belt around the waist. The patient swallows the capsule and it travels through the GI tract by normal peristaltic waves, capturing images of the inner lining of the GI tract. As it continues down the GI tract, the images captured may identify potential abnormalities, such as obscure GI bleeding, suspected small intestinal tumors and surveillance in patients with polyposis syndromes and chronic diarrhea. During this procedure, the WCE captures images and the capsule is later excreted naturally.

A number of technical challenges regarding size and cost, energy requirements, and wireless communication technology of WCEs are under investigation and in the heart of these investigations is the fundamental unsolved challenge of WCE navigation and localization. The knowledge of location and orientation of the capsule enables the physician to localize and assess the lesion, abnormalities or pathologies to recommend next steps in the patient's treatment. Various challenges are raised by highly inhomogeneous human body medium that are profoundly different from the traditional indoor radio propagation challenges. Effects such as increased dampening, scattering, multipath and variable RF speed present to a much larger degree when the RF wave travels through different body media (e.g. bone, muscle, fat and blood) with varying dielectric properties. The problem gets even more challenging by the gastrointestinal movement, filling and emptying cycle, resulting in unpredictable ranging error. In addition, adhesions, bleeding, diseases and filling and emptying cycle alter GI tract motility causing a nonlinear time-variant motion in the GI tract especially between pylorus and ileocecal valve. Therefore, understanding of radio propagation inside human body is of great importance.

Various technologies for localization of the WCE have been explored in feasibility studies; including ultrasound [2], magnetic tracking [3] and computer vision [4]. In [2], a method of tracking a WCE inside the GI tract based on the application of a microcontroller to control the generation and transmission of ultrasonic pulses was presented. In [3], a tracking system consisting of a magnetic marker, a sensor array, amplifiers, data acquisition devices and a signal processing unit was designed. In [4], a low-complex and efficient image compression method, based on integer-to-integer 4x4 DCT transform was presented and experimentally verified. Among these technologies, RF signal based localization systems have the advantage of application-non-specific and relatively inexpensive hardware implementation. RF capsule localization systems usually use an external sensor array that measures the RF signal metrics

Research supported by University of Southern Denmark.

Esmaeil S. Nadimi is with the Faculty of Engineering, University of Southern Denmark, Campusvej55, 5230 Odense, DK (corresponding author to provide phone: 0045-2778-1929; e-mail: esi@ mmmi.sdu.dk).

Victoria Blanes-Vidal is with the Faculty of Engineering, University of Southern Denmark, Niels Bohrs Alle 1, 5230 Odense, DK (e-mail: vbv@ kbm.sdu.dk).

Vahid Tarokh is with the School of Engineering and Applied Sciences (SEAS), Harvard University, 33 Oxford St, Cambridge, MA 02138 USA, (e-mail: vahid@seas.harvard.edu).

Per Michael Johansen is with the Faculty of Engineering, University of Southern Denmark, Niels Bohrs Alle 1, 5230 Odense, DK (e-mail: pmj@ tek.sdu.dk).

978-1-4244-7929-0/14/$26.00 ©2014 IEEE

of capsule transmissions at multiple points and uses this information to estimate the distance or uses fingerprinting algorithms to estimate the location of the capsule. The RF localization technique based on time or angle measurement methods, i.e., Time of Arrival, Time Difference of Arrival and Angle of Arrival are not feasible. The strong absorption of human tissue causes large ranging errors and the limited bandwidth of the Medical Implant Communication Services (MICS) band make high resolution TOA estimation difficult.

In this work, we consider the problem of source localization in inhomogeneous transmission media by constraint-based Bayesian inference approach using RSS profiling method that accounts for Rayleigh fading, variable path-loss exponent and uncertainty in location information received from the neighboring nodes and anchors. We derive a Bayesian-based localization approach to estimate the unknown location of a node in a network given the coarse information of RSS measurements and the position estimate of some neighboring nodes (anchors) with uncertain location information as expected from most real-world applications.

The rest of the paper is organized as follows. In section II, problem statement, formulation and basic assumptions and the new developed constraint-based Bayesian inference localization method using RSS measurements are presented. Section III describes the simulation results, and the discussions and the conclusions of this study are presented in section IV.

II. Problem Formulation and Algorithm Development

A. Signal Strength-based Measurement Model

Assume a sensor network in $\Re^3$ with m anchors and n sensors. An anchor is defined as a node whose location $a_k = \left[x_{a_k}, y_{a_k}, z_{a_k}\right]^T, k = 1, \cdots, m$ is known with uncertainty defined by a probability density function (pdf) $f_{a_k}(x_{a_k}, y_{a_k}, z_{a_k})$ and a sensor node is a node whose location $s_i = \left[x_{s_i}, y_{s_i}, z_{s_i}\right]^T, i = 1, \cdots, n$ needs to be estimated using a pdf function $f_{s_i}(x_{s_i}, y_{s_i}, z_{s_i})$. If an anchor at a_k emits a signal of power P_{TX}, the strength of the received signal P at sensor location s_i can be calculated in the log-scale as the following:

$$P(d_{ik}) = \overline{P}(d_{ik}) + X_\Omega \quad s.t. \ \overline{P} = P_0 + 10\,n\log(d_{ik}) \tag{1}$$

where P, $\overline{P}$ and P_0 denote the random variable RSS (dB), the mean value of RSS measurements at a given distance and the RSS measurements at a reference distance, respectively. d_{ik} is the distance between any two given nodes, X_Ω is a random variable caused by shadowing and fading effects and n is the path-loss exponent. Due to the inhomogeneity of the transmission interface, we assume a Rayleigh distribution over $X_\Omega \sim (\Omega)$ rather than a Gaussian distribution or Rician distribution (fading). Additionally, due to the variations of the path-loss exponent throughout the inhomogeneous medium between any two given points in the network, we assume a Gamma distribution over n independent from X_Ω with the scale and shape parameter θ and η respectively, $n \sim Gamma\ (\eta, \theta)$ [5].

Proposition 1: consider model (1) and let X_Ω and n be two independent random variables with Rayleigh distribution and Gamma distribution, respectively. The pdf of d_{ij} given a value P can be approximated as follows:

$$f\left(d_{ij}\middle|P\right) = \alpha d_{ij}^{-(\eta+2)}\left(\Psi_{\eta+2}(d_{ij}) + (P - P_0)\Psi_{\eta+1}(d_{ij})\right) \tag{2}$$

$$\Psi_\eta(d_{ij}) = \Omega^{-\eta}\Gamma(\eta)\exp\left(4\Omega^2\left(\beta + \frac{1}{\theta d_{ij}}\right)^2\right)D_{-\eta}\left(\Omega(\beta + \frac{1}{\theta d_{ij}})\right) \tag{3}$$

$$\alpha = \left(\Omega^2\theta^\eta\Gamma(\eta)\right)^{-1}\exp\left(-\frac{\beta^2\Omega^2}{2}\right), \beta = \frac{P - P_0}{\Omega^2}, \Gamma(\eta) = \int_0^\infty t^{\eta-1}e^{-t}dt$$

In model (3), $D_\eta(z)$ denotes the parabolic-cylinder function. For the proof of proposition 1, the reader is referred to the section Appendix.

B. Bayesian-based localization method

Assume that the sensor node i receives a beacon packet from an anchor. The updated location pdf of sensor i, $f_{s_i}^{update}(x_{s_i}, y_{s_i}, z_{s_i})$, can be estimated using Bayesian inference by intersecting the current location pdf of the sensor i, $f_{s_i}(x_{s_i}, y_{s_i}, z_{s_i})$, and RSS measurement pdf (2) between the sensors i and anchor k transmitting the beacon packet.

$$f_{s_i}^{update}(x_{s_i}, y_{s_i}, z_{s_i}) = \frac{f_{s_i}(x_{s_i}, y_{s_i}, z_{s_i})\Phi(x_{s_i}, y_{s_i}, z_{s_i}|P)}{\oint_{V_i} f_{s_i}(x_{s_i}, y_{s_i}, z_{s_i})\Phi(x_{s_i}, y_{s_i}, z_{s_i}|P)dV_i}$$

$$= \frac{f_{s_i}(x_{s_i}, y_{s_i}, z_{s_i})\Phi(x_{s_i}, y_{s_i}, z_{s_i}|P)}{\int_{y_{s_i,\min}}^{y_{s_i,\max}}\int_{x_{s_i,\min}}^{x_{s_i,\max}}\int_{z_{s_i,\min}}^{z_{s_i,\max}} f_{s_i}(x_{s_i}, y_{s_i}, z_{s_i})\Phi(x_{s_i}, y_{s_i}, z_{s_i}|P)dx_{s_i}dy_{s_i}dz_{s_i}} \tag{4}$$

In (4), V_i denotes the network volume of possible locations of sensor i ranging from $\left[x_{s_i,\min}, y_{s_i,\min}, z_{s_i,\min}\right]$ to $\left[x_{s_i,\max}, y_{s_i,\max}, z_{s_i,\max}\right]$. Furthermore, Φ is the pdf constraint imposed on the location of sensor i given the RSS measurement pdf (2) and the location pdf of the transmitting node.

$$\Phi(x_{s_i}, y_{s_i}, z_{s_i}, x_{a_k}, y_{a_k}, z_{a_k}|P) = \frac{\oint_{V_k} f(d_{ik}|P)f_{a_k}(x_{a_k}, y_{a_k}, z_{a_k})dV_k}{\oint_{V_i}\oint_{V_k} f(d_{ik}|P)f_{a_k}(x_{a_k}, y_{a_k}, z_{a_k})dV_k dV_i} \tag{5}$$

$$= \frac{\int_{y_{a_k,\min}}^{y_{a_k,\max}}\int_{x_{a_k,\min}}^{x_{a_k,\max}}\int_{z_{a_k,\min}}^{z_{a_k,\max}} f(d_{ij}|P)f_{a_k}(x_{a_k}, y_{a_k}, z_{a_k})dx_{a_k}dy_{a_k}dz_{a_k}}{\int_{y_{s_i,\min}}^{y_{s_i,\max}}\int_{x_{s_i,\min}}^{x_{s_i,\max}}\int_{z_{s_i,\min}}^{z_{s_i,\max}}\int_{y_{a_k,\min}}^{y_{a_k,\max}}\int_{x_{a_k,\min}}^{x_{a_k,\max}}\int_{z_{a_k,\min}}^{z_{a_k,\max}} f(d_{ij}|P)f_{a_k}(x_{a_k}, y_{a_k}, z_{a_k})dx_{a_k}dy_{a_k}dz_{a_k}dx_{s_i}dy_{s_i}dz_{s_i}}$$

in which V_k denotes the network volume of possible locations of anchor k ranging from $[x_{a_k,\min}, y_{a_k,\min}, z_{a_k,\min}]$ to $[x_{a_k,\max}, y_{a_k,\max}, z_{a_k,\max}]$. Coordinates $[x_{s_i}, y_{s_i}, z_{s_i}]$ that maximizes $f_{s_i}^{update}(x_{s_i}, y_{s_i}, z_{s_i})$ in (6) corresponds to the estimated locations of sensor i.

$$[\hat{x}_{s_i}, \hat{y}_{s_i}, \hat{z}_{s_i}] = \arg\max_{x_{s_i}, y_{s_i}, z_{s_i}} (f_{s_i}^{update}(x_{s_i}, y_{s_i}, z_{s_i})) \quad (6)$$

III. ALGORITHM IMPLEMENTATION AND SIMULATION RESULTS

A. Simulation Results

To evaluate the performance of the Bayesian-based localization algorithm, various examples featuring different values for sensor and anchor locations, anchor location uncertainty, number of anchors covering the sensor and the characteristics of the inhomogeneous transmission medium are provided. For simulation purposes, the mode parameter of the Rayleigh fading between the sensor and any anchor was set to 4.5 ($\Omega = 4.5$ cm^3). In addition, the path-loss exponent of the inhomogeneous medium n was set to $n \sim Gamma(4,1)$. The pdf of the distance given P-P0 (dB) between the sensor and any anchor is presented in Fig. 1(a) and the mean and one time standard deviation of the simulated RSS (P-P0) at each distance are shown in Fig. 1(b)

Example1. Assume a 2-D scenario in which the sensor s_1 is a stationary node located at [1.5 1 0] and $f_{a_k}(x_{a_k}, y_{a_k}, z_{a_k}), k = 1,2,\cdots,5$ has Gaussian distribution with mean (cm) μ_{a1}=[2.5 3 0], μ_{a2}=[-0.5 -1 0], μ_{a3}=[0.5 2 0], μ_{a4}=[3.5 0 0] and μ_{a5}=[1 0 0] and standard deviation (cm) σ_{a1}=[0.3 0.3 0], σ_{a2}=[0.3 0.3 0], σ_{a3}=[0.3 0.3 0], σ_{a4}=[0.3 0.3 0], σ_{a5}=[0.2 0.4 0] . Location estimation for the network topology using beacon packets from a set of 5 anchors (a_1, a_2, a_3, a_4, a_5) after only one iteration in the x-y plane is presented in Fig. 2. Final position estimation of $\hat{s}_1$ is computed as the intersection of the pdf estimation of the location constraint imposed by anchors a_1, a_2, a_3, a_4 and a_5.The uncertainty in the information of location of each anchor is presented by contours around the anchor. The center of the contour represents the estimated location of the node with the highest probability (after maximizing the index in Eq. (6)) and the radius of the outermost contour is 1-σ elliptical error bound. In this example, the true and the estimated location of s_1 were [1.5 1 0] and $\hat{s}_1$ [1.42 0.94 0], respectively. As a result, the estimation error of approximately 0.10 in the x-y plain is small compared to the confidence bounds on the error.

Example 2. Assume a 3-D scenario in which the sensor s_1 is a stationary node located at [-1 0 1] and $f_{a_k}(x_{a_k}, y_{a_k}, z_{a_k}), k = 1,2,\cdots,5$ has Gaussian distribution with mean (cm) μ_{a1}=[1 1 1], μ_{a2}=[-2 -1 0], μ_{a3}=[-3 2 0], μ_{a4}=[0 -2 1] and μ_{a5}=[0 0 0.5] and standard deviation (cm) σ_{a1}=[0.3 0.3 0.3], σ_{a2}=[0.3 0.3 0], σ_{a3}=[0.3 0.3 0.3], σ_{a4}=[0.3 0.3 0], σ_{a5}=[0.2 0.4 0.3] . Location estimation for the network topology using beacon packets from the set of 5 anchors (a_1, a_2, a_3, a_4, a_5) after only one iteration in the x-y-z space is carried out and the true and the estimated location of s_1 were [-1 0 1] and $\hat{s}_1$ [-0.85 0.1 0.9], respectively. As a result, the estimation error of approximately 0.21 is small compared to the confidence bounds on the error (approximately 0.30).

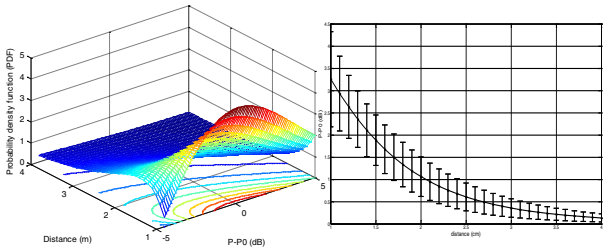

(a) (b)

Figure 1. (a) The pdf of distance given P-P0 between the sensor and any anchor. (b) Mean and one time standard deviation of the simulated RSS (P-P0) at each distance.

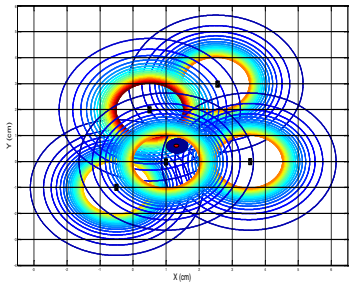

Figure 2. Contours of the location estimation for the network topology using a set of 5 anchors. Sensor and the anchors and are marked by circle and rectangles, respectively. The contour around the sensor represents the constraint on the location of the sensor imposed by the anchors (Example 1).

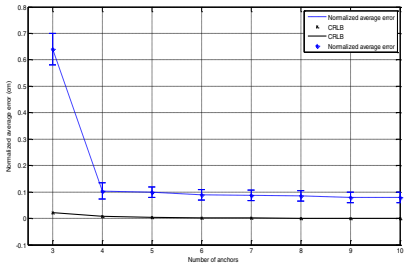

Figure 3. Effect of number of anchors on localization accuracy

The effect of number of anchors on the localization accuracy of the Bayesian-based approach is presented in Fig. 3. In addition, the Cramer-Rao lower bound (CRLB) is evaluated, showing a close performance of the Bayesian-based approach to the optimum (CRLB). We remark that the CRLB shown is calculated assuming full connectivity, and as

such provides only a loose lower bound on the best performance achievable by any unbiased estimator.

B. Discussions and future works

It can be observed from the uncertainty contours of the sensor and anchor locations in Fig. 2 that the uncertainty in the sensor location estimation was significantly smaller compared to that of anchors and the RSS measurements. In addition, the localization error obtained by the Bayesian-based localization method using RSS measurements was larger when the sensor was outside the convex hull of the anchors compared to when the sensor laid inside the convex hull of the anchors. Furthermore, to deploy the RSS fingerprinting method in real terrains such as GI tract monitoring, some parameters of Eq. (2) such as P, $\overline{P}$, P_0, Ω, θ and η corresponding to the human body medium should be estimated prior to the estimation of the probability model.

The robustness analysis of the Bayesian inference methods study the sensitivity of the Bayesian answers to uncertain inputs (the model or likelihood and the prior distribution). In this study, the likelihood refers to the pdf constraint $\Phi(x_{s_i}, y_{s_i}, z_{s_i}, x_{a_k}, y_{a_k}, z_{a_k} | P)$ imposed on the location of a node given the RSS measurement pdf (2). Several studies have investigated the impact of different priors (informative vs. non-informative) on the performance robustness of the Bayesian inference-based methods ([6-7]) which suggest that informative priors significantly reduce the sensitivity of the Bayesian-based methods to outliers and model uncertainty in deriving posterior distributions. In this study, Gaussian distribution (informative) as *a priori* information of the anchors' locations pdf $f_{a_k}(x_{a_k}, y_{a_k}, z_{a_k})$ and nodes' location pdf $f_s(x_s, y_s, z_s)$ were selected resulting in a robust localization method to the variations of the model (likelihood) and the terrain characteristics.

The performance of the Bayesian-based method using RSS measurements in terms of root mean square localization error (RMSE) after running 1000 Monte Carlo simulation trials were evaluated (1.6mm) and compared to the generated RMSE of other localization approaches (e.g. the classical MDS (64.2mm) [8], MLE (32.2mm) [8], dwMDS (36.3mm) [9] and POCS (2.3mm) [10]) when a sensor node was covered by five anchors in a 3-D terrain. The RMSE of the location estimation obtained using the Bayesian-based method using RSS measurements were significantly smaller than those of other methods showing improvements in the location estimation.

As part of the future work, we intend to measure dielectric properties of human body and specifically the GI tract to test the developed model and the performance of the developed Bayesian method in WCE navigation and localization.

APPENDIX

The pdf of $\log(d_{ij})$ given P can be formulated as follows:

$$\log(d_{ij}) = \frac{P_0 - P + X_\Omega}{10n} \tag{1a}$$

$$f_{\log(d_{ij})}(y) = \int_{-\infty}^{\infty} |x| f_{(P_0 - P + X_\Omega)}(xy) f_{10n}(x) dx$$

Given the pdf of X_Ω and n as following, the pdf of $\log(d_{ij})$ can be calculated:

$$f_{X_\Omega}(x) = \frac{x}{\Omega^2}\exp\left(-\frac{x^2}{2\Omega^2}\right), \quad f_n(x,\eta,\theta) = \frac{\theta^{-\eta}}{\Gamma(\eta)} x^{\eta-1}\exp(-\frac{x}{\theta}) \qquad x \in [0,\infty) \tag{2a}$$

$$f_{\log(d_{ij})}(y) = \int_0^\infty x^\eta \left(\frac{xy + P - P_0}{\Omega^2}\right)\exp\left(-\frac{(xy + P - P_0)}{2\Omega^2} - \frac{x}{\theta}\right)\frac{10\theta^{-\eta}}{\Gamma(\eta)} dx$$

$$= \frac{10}{\Omega^2\theta^\eta\Gamma(\eta)}\int_0^\infty x^\eta (xy + P - P_0)\exp\left(-\frac{(xy + P - P_0)^2}{2\Omega^2} - \frac{x}{\theta}\right)dx$$

$$= \frac{10}{\Omega^2\theta^\eta\Gamma(\eta)}\int_0^\infty x^{\eta+1} y\exp\left(-\frac{(xy + P - P_0)^2}{2\Omega^2} - \frac{x}{\theta}\right)dx + \frac{10(P - P_0)}{\Omega^2\theta^\eta\Gamma(\eta)}\int_0^\infty x^\eta \exp\left(-\frac{(xy + P - P_0)^2}{2\Omega^2} - \frac{x}{\theta}\right)dx$$

$$= \frac{10}{\Omega^2\theta^\eta\Gamma(\eta)}\int_0^\infty \frac{z^{\eta+1}}{y^{\eta+1}}\exp\left(-\frac{(z + P - P_0)^2}{2\Omega^2} - \frac{z}{\theta y}\right)dz + \frac{10(P - P_0)}{\Omega^2\theta^\eta\Gamma(\eta)}\int_0^\infty \frac{z^\eta}{y^{\eta+1}}\exp\left(-\frac{(z + P - P_0)^2}{2\Omega^2} - \frac{z}{\theta y}\right)dz$$

$$= \frac{10\exp\left(-\frac{(P - P_0)^2}{2\Omega^2}\right)}{\Omega^2\theta^\eta\Gamma(\eta)y^{\eta+1}}\int_0^\infty z^{\eta+1}\exp\left(-\frac{z^2}{2\Omega^2} - z\left(\frac{2(P - P_0)}{2\Omega^2} + \frac{1}{\theta y}\right)\right)dz$$

$$+ \frac{10(P - P_0)\exp\left(-\frac{(P - P_0)^2}{2\Omega^2}\right)}{\Omega^2\theta^\eta\Gamma(\eta)y^{\eta+1}}\int_0^\infty z^\eta \exp\left(-\frac{z^2}{2\Omega^2} - z\left(\frac{2(P - P_0)}{2\Omega^2} + \frac{1}{\theta y}\right)\right)dz$$

and (2) follows readily.

REFERENCES

[1] American Cancer Society. Colorectal cancer facts and figures, 2008-2010.

[2] K. Arshak and F. Adepoju. Capsule Tracking in the GI Tract: A Novel Microcontroller based Solution. SAS 2006 – *IEEE Sensors Applications Symposium* Houston, Texas USA, 7 - 9 February 2006.

[3] J. Hou, Y. Zhu, L. Zhang, Y. Fu, F. Zhao, L. Yang, and G. Rong. Design and Implementation of a High Resolution Localization System for In-vivo Capsule Endoscopy. 2009 *Eighth IEEE International Conference on Dependable, Autonomic and Secure Computing*.

[4] J. Bulat, K. Duda, M. Duplaga, R. Fraczek, A. Skalski, M. Socha, P. Turcza, and T. P. Zielinski, "Data Processing Tasks in Wireless GI Endoscopy: Image-Based Capsule Localization & Navigation and Video Compression". Engineering in Medicine and Biology Society, 2007. EMBS 2007. *29th Annual International Conference of the IEEE*. Aug. 2007 pp. 2815 – 2818.

[5] Larsen, J. and Green, O. and Nadimi, E. S. and Steftgaard, T., "The Effect on Wireless Sensor Communication When Deployed in Biomass Sensors", *Sensors* , Vol. 11, Nr. 9, 25.08.2011.

[6] Y. Chen, and D. Fournier, "Impacts of atypical data on Bayesian inference and robust Bayesian approach in fisheries". *Canadian Journal of Fisheries and Aquatic Sciences* (1999) Volume: 56, Issue: 9, Pages: 1525-1533

[7] J. Berger, "An Overview of Robust Bayesian Analysis" (1993). Technical Report # 93-53C

[8] N. Patwari, A. O. Hero, M. Perkins, N. S. Correal, and R. J. O'Dea, "Relative location estimation in wireless sensor networks," *IEEE Trans. Signal Process.*, vol. 51, no. 8, pp. 2137–2148, Aug. 2003.

[9] J. A. Costa, N. Patwari, A. O. Hero, "Distributed Weighted-Multidimensional Scaling for Node Localization in Sensor Networks". *ACM Transaction on sensor networks*, vol. 2, no. 1, pp. 1-26, 2006.

[10] A. O. Hero, and D. Blatt, "Sensor network localization via projection onto convex sets (POCS)," in *Proc. ICASSP*, Mar. 2005, vol. 3, pp. 689–692.